# New method for side pumping of double-clad fiber lasers using planar grating written into the inner cladding

Xingchun Chu*, Shanghong Zhao, Zhuoliang Wu, Lei Shi, Shengbao Zhan, Yunxia Li, Lihua Ma
Department of network Engineering, Telecommunication Engineering Institute, AFEU, Xi'an, Shaanxi 710077, China

## ABSTRACT

A new side pumping method based on the diffractive properties of a planar grating which is directly written into the inner cladding of a double-clad fiber (DCF) is proposed. This technique assumes that the inner cladding of the DCF is highly photosensitive and its diameter is large enough. Then a planar grating with a proper thickness can be written into the inner cladding. The principles, characteristics and coupling efficiencies of the proposed scheme are described and simulated by coupled wave theory. The simulating results show that the coupling efficiencies can achieve over 98% for TE-, TM- and un-polarized incident pump lights simultaneously. And the average coupling efficiencies can still achieve 80% regardless of TE or TM polarization even when the pump wavelength ranges from 974 to 978nm and the incident angle ranges from −0.8° to 0.8°. The fabrication tolerances of the planar grating and the leakage of pump powers for multi-point side-pumping are also analyzed. The advantages of the proposed scheme include: (1) no risk of damaging the DCF; (2) no index-matching optical adhesive; (3) high temperature sustainability; (4) simple, stable and compact. It provides an effective way to scale the output power of DCF lasers or amplifiers to a high level.

**Keywords:** Laser diode, Fiber lasers, Side-pumping, Photosensitive inner cladding, Planar grating

## 1. Introduction

Diode-pumped rare-earth-doped (RE-doped) fiber laser is a potential candidate of high-efficient high-power coherence source, which have many applications in optical-communications, material processing and bio-physics. Since double-clad fiber (DCF) can provide larger cross-section and numerical aperture, it has been applied extensively for high-power fiber lasers. The limitation of the output power generated by DCF lasers are determined principally by how much pumping light can be launched into the fiber[1].

The pumping approaches for DCF reported so far can be divided into two groups: the end-pumping and side-pumping schemes[2]. End-pumping is straightforward and efficient method to couple the pump light into the inner cladding of DCF. However, this pump regime has some obvious disadvantages. First, it denies the accessibility to the ends of the fiber for coupling the input signal and extracting the amplified output in the fiber amplifier applications. Second, since the pump laser diodes are limited in power and brightness, the output power cannot be scaled without increasing the cladding size[3]. Side-pumping is attractive, because it overcomes the mentioned undesirable effects and there is no principal upper limit to the launchable pump power. In the past, several side-pumping techniques have been developed for launching high-power pump light into the DCF through its side. V-groove side-coupling technique[3] and embedded-mirror method[4][5] are scalable but quite delicate, complicate and imply the risk of damaging the fiber. Other methods, such as angle-polished method[6][7], micro-prism side-coupler[8], fused fiber coupler[9] and diffraction-grating method[10][11][12], etc, do not need to cut or polish the inner cladding of DCF but require index matched optical adhesive to adhibit the coupling structure to the surface of the inner cladding. And the coupling efficiencies of these side-pumping techniques are seriously affected by the optical, mechanical and thermal properties of the optical adhesive. So, it is indispensable to develop new simple, efficient, stable and compact side-pumping techniques in order to scale the power output of single DCF lasers.

The advent of photosensitive fiber makes it possible to directly write Bragg gratings into the fiber core for constructing compact fiber lasers. Several types of doped silica materials have been developed to fabricate highly photosensitive fibers, including Sb/Ge-codoped fiber[13], Bi/Ge-codoped fiber[14], B/Ge-codoped fiber[15], etc. These fibers have high photosensitivity and good temperature sustainability up to several hundred degrees. Furthermore, uniform index modulation over the inner cladding region was realized by utilizing highly photosensitive B/Ge-codoped fiber[16].

International Symposium on Photoelectronic Detection and Imaging 2009: Laser Sensing and Imaging,
edited by Farzin Amzajerdian, Chun-qing Gao, Tian-yu Xie, Proc. of SPIE Vol. 7382, 73820X
 · doi: 10.1117/12.834164

In this paper a novel side-pumping technique is proposed to launch high power pump light into the inner cladding of a DCF. The proposed method assumes that the inner cladding of a DCF is photosensitive and its radius is large enough to allow planar grating with proper thickness being written into it. The pump sources can be brought into close proximity to the grating without intervening optical element, and pump beams are launched into the inner cladding by efficient diffraction of the planar grating. High coupling efficiencies can be achieved due to the excellent diffractive property of the designed planar grating. Instead of adding an additional diffraction-grating structures to the DCF[10][11], this technique can be implemented just by modulating the refractive index of some part of the inner cladding through UV radiation and an all-fiber laser can be realized. Compared to the aforementioned side-pumping methods, this technique is more simple, stable and compact. In particular, the risk for damaging the DCF is avoided and index-matching optical adhesive is no longer needed.

## 2. Side-pumping Principle

If the core of a DCF is surrounded by highly photosensitive B/Ge-doped inner cladding, index modulation over the inner cladding would be possible and planar grating with a certain thickness could be written into it by exposure of the fiber to ultraviolet emission. Although the germanium doping increases the refractive index of silica, the boron doping lowers it, the same refractive index as that of pure silica can be achieved for the inner cladding[15]. And the Er/Yb codoped core can not be affected by the B/Ge-doped inner cladding.

Fig. 1 shows the basic idea of the side-pumping scheme by a planar grating written into the square photosensitive inner cladding of a DCF. The outer cladding and jacket of a short section of the DCF is removed and the inner cladding is exposed. A planar grating is directly written into the photosensitive inner cladding by UV emission. As can be seen, the DCF does not need to be polished and no other element is adhibited to it. The thickness of the planar grating is $h$. In order not to disturb the core, the maximal thickness $h_{max}$ of the planar grating should be confined to less than $(a-d)/2$, where $a$ and $d$ are the length of side of the inner cladding and diameter of the core, respectively. The pump light of a high-power diode-bar collimated by a cylindrical lens incident on the planar grating. They will be efficiently diffracted if they satisfy the Bragg condition of the planar grating. The diffracted beam will be guided in the DCF if the angle $\theta$ with respect to the interface between the inner and outer cladding is smaller than the critical angle of total internal reflection $\theta_{max}$. It means that the diffractive angle $\phi = \pi/2-\theta$ of the diffracted beam have to be larger than $(\pi/2-\theta_{max})$. Therefore total internal reflection will occur at the inner-outer cladding interface until the pump lights are absorbed completely.

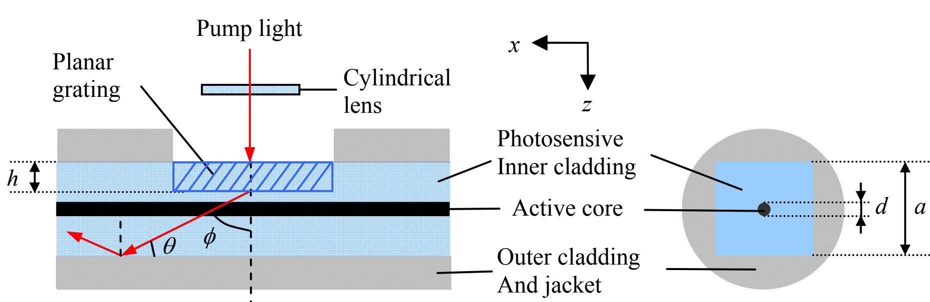


Fig.1 The basic idea of the side-pumping scheme by the planar grating written into the square photosensitive inner cladding of a DCF

Since the planar grating is directly written into the photosensitive inner cladding by UV emission, this side-pumping scheme is simple and needs not to cut or angle polish the DCF as should be done for the V-groove side-coupling[3] or embedded-mirror method[4]. The risk of damaging the fiber is avoided. Furthermore, index-matching optical adhesive, which can not sustain too high temperature due to its heat absorption property, is no longer needed. The power sustainability can be enhanced because of the good temperature sustainability of the photosensitive B/Ge-doped inner cladding.

## 3. Numerical Simulation of Pump Coupling Efficiency

For analyzing the coupling efficiency of the proposed side-pumping scheme, a DCF with a 20$\mu m$ active core and a square photosensitive B/Ge-doped inner cladding whose length of side is 300$\mu m$ and numerical aperture of 0.4 is considered. The refractive index of the inner cladding is assumed to be the same of fused silica ($n_{silica}$= 1.453) at $\lambda$=976*nm[8]*. And the amplitude of the photoinduced index changes of the inner cladding is chosen to be as great as $\Delta n = 2\times10^{-3}$ [15]. Moreover, we assume that a UV-induced index perturbation is sinusoidal across the given section of the inner cladding and the grating is lossless. The medium upside the planar grating is air ($n_{air}$= 1) and that downside is photosensitive inner cladding due to the confined $h_{max}$. The critical angle of total internal reflection $\theta_{max}$ is 16°. It requires that the diffractive angle $\phi$ must be larger than 74°. In order to determining the grating vector, Fig.2 shows a vector diagram of the transmission planar grating for Bragg incidence. The $\boldsymbol{\rho}$ and $\boldsymbol{\delta}$ are the propagation vectors of the incident pumping wave and diffracted wave respectively and **K** is the grating vector. The *z*-axis is chosen in the plane of incidence and perpendicular to the DCF, the *x*-axis parallel to the DCF and the *y*-axis perpendicular to the paper. The fringe planes are perpendicular to the plane of incidence and slanted with respect to the *z*-axis at an angle $\varphi$. According to the Bragg condition of coupled-wave theory[18], the boundary angle requires a grating period $\Lambda$ between 475 and 558*nm* at a wavelength of 976*nm*. A grating period $\Lambda$ of 512*nm* and a slant angle $\varphi$ of 49° are selected, and the corresponding Bragg diffraction angle is 82°.

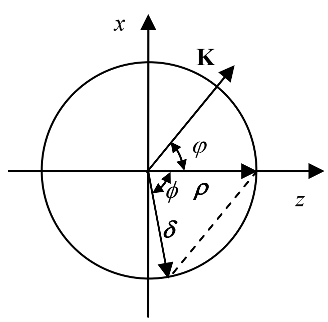

Fig.2 Vector diagram for Bragg incidence

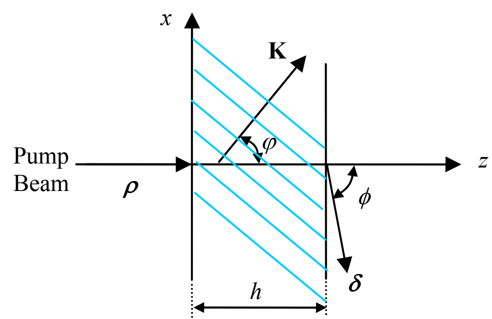

Fig.3 Geometry for planar grating diffraction

The coupled wave theory is used to analyze the coupling efficiencies of the pump light. In the coupled-wave theory, the infinite length of grating is assumed. However, the proposed grating structure has a finite length, which is 1.1*cm* in order to match the length of the output beam of the LD bar[10]. Because the period $\Lambda$ and the length $L$ of our proposed grating structure is 512$^{nm}$ and 1.1$^{cm}$, respectively, the number-of-periods N is equal to 21,484, which is enough large to ignore the effect of the finite length of the grating on the accuracy of the results. Moreover, in order to assure the validity of the coupled wave theory, the minimum thickness is chosen to be $h_{min} = 10 n_{silica}\Lambda^2 / 2\pi\lambda = 622nm$ in the following simulation according to the equation (75) of Ref. [18].

Fig.3 shows the geometry for planar transmission grating diffraction. For TE polarization, the diffraction efficiencies of lossless dielectric grating is[18]

$$\eta_{TE} = \sin^2\left(\nu^2 + \xi^2\right)^{1/2} \Big/ \left(1 + \xi^2/\nu^2\right) \tag{1}$$

And

$$\nu = \pi\Delta n h \Big/ \lambda\left(c_R c_S\right)^{1/2} \tag{2}$$

$$\xi = \vartheta h / 2c_S \tag{3}$$

Where $c_R = \cos\alpha$ .The obliquity factor $c_S = c_R - K\cos\varphi/\beta$ , the dephasing measure $\vartheta = K\cos(\varphi-\alpha) - \lambda K^2 / 4\pi n_{silica}$ , the amplitude of the grating vector $K = 2\pi/\Lambda$ and $\beta = 2\pi n_{silica}/\lambda$ .

For TM polarization, equation (2) should be modified as follow

$$\nu = -\pi \Delta n h \cos(\phi_0 - \varphi) \Big/ \lambda (c_R c_S)^{1/2} \tag{4}$$

Where $\phi_0$ is the Bragg angle.

Fig. 4 shows the diffraction efficiencies against thickness of the planar grating for TE- and TM-polarized wave. The maximum thickness $h_{\max}$ of the grating is confined to 140$\mu m$. It reveals that the maximum diffraction efficiency for TE- and TM-polarized wave can not simultaneously achieve 100% at the same thickness. A trade-off for the thickness of the grating must be made in order to achieve an optimized efficiency because the pump light is un-polarized. Thus, an optimum thickness is chosen to be 106.1$\mu m$ and the diffraction efficiencies for TE, TM and un-polarized wave (its efficiency is $(\eta_{TE}+\eta_{TM})/2$) are all about 98.1%.

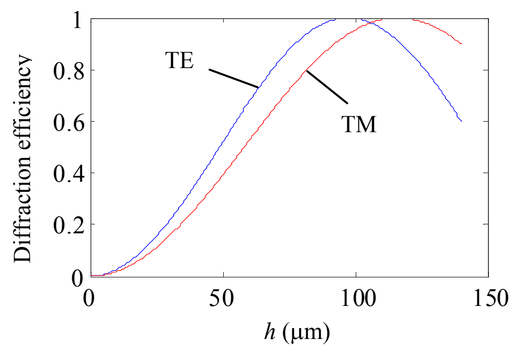


Fig.4 The diffraction efficiencies against thickness of the planar grating

Figs. 5 shows the wavelength and angular selectivity of the grating when the above parameters are considered. The full width half maximum (FWHM) bandwidth of the wavelength selectivity is about 5.5*nm* and that of the angular selectivity is about 1.6°(28*m*rad). As can be seen, the diffraction efficiencies for TE- and TM-polarized wave are almost the same in the main lobe no matter what the wavelength or angle of incidence changes, respectively. The diffraction efficiencies in side lobe, however, show a little difference between TE- and TM-polarized wave.

To maximize pump absorption, the pump diode can be temperature tuned to center its 3*nm* wide emission on the 10*nm* wide Yb absorption peak at 976*nm*[3]. And we suppose that the total pump power is uniformly distributed in the all incident wavelengths and angles. The total impact of variations of the incident wavelengths and angles on the final pump coupling efficiencies is showed in Fig.6. The profiles of the diffraction efficiencies for TE- and TM-polarized wave are almost the same. And the average diffraction efficiencies can achieve 76.86% regardless of TE- or TM- polarization

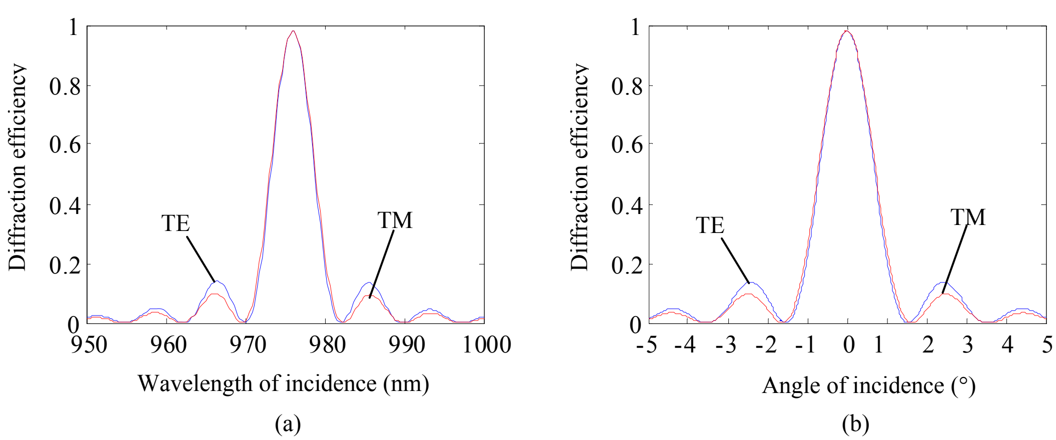


Fig.5 The (a) wavelength and (b) angular selectivity of the designed planar grating

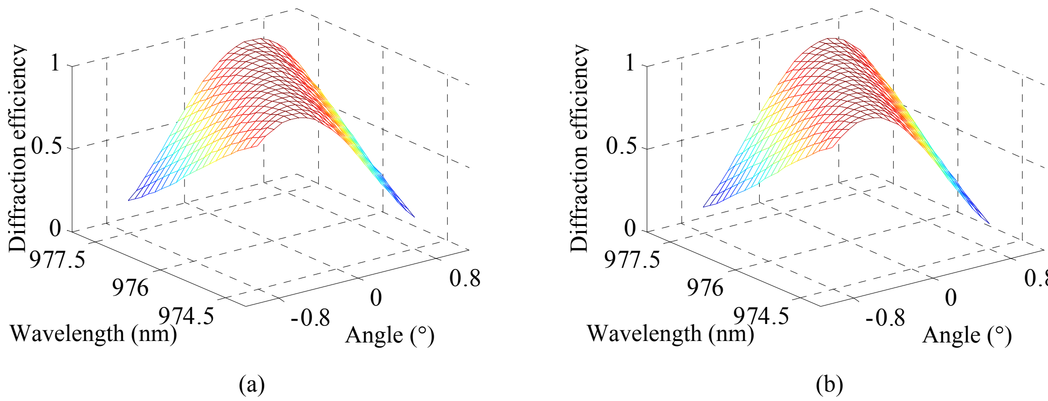


Fig.6 Diffraction efficiencies vs. incident points wavelength and angle for (a) TE- (b) TM-polarized

when the pump wavelength ranges from 974.5 to 978.5*nm* and the incident angle ranges from −0.8° to 0.8°.

## 4. Tolerance Analysis

The coupling efficiencies are simulated to evaluate the total impact of variations of the period and thickness of the grating on the final pump coupling efficiency. The simulation results are shown in Fig.7 for different polarization states. In the two cases, the contour lines of the coupling efficiencies are oval and symmetric when the period is 512*nm*. And the areas of the highest efficiencies are approximately the same size. The tolerance of period for TE-polarized is larger than that for TM-polarized while the tolerance of thickness for TE-polarized smaller than that for TM-polarized. The results indicate that the coupling efficiency is more sensitive to the variations of the period than the thickness of the planar grating. When the tolerance of the period is confined to 512±2*n*m, the coupling efficiencies higher than 80% can be achieved when the thickness ranges from 80 to 130$\mu m$. Thus, it is clear that the written error tolerance of the thickness is loose while that of the period is a little strict.

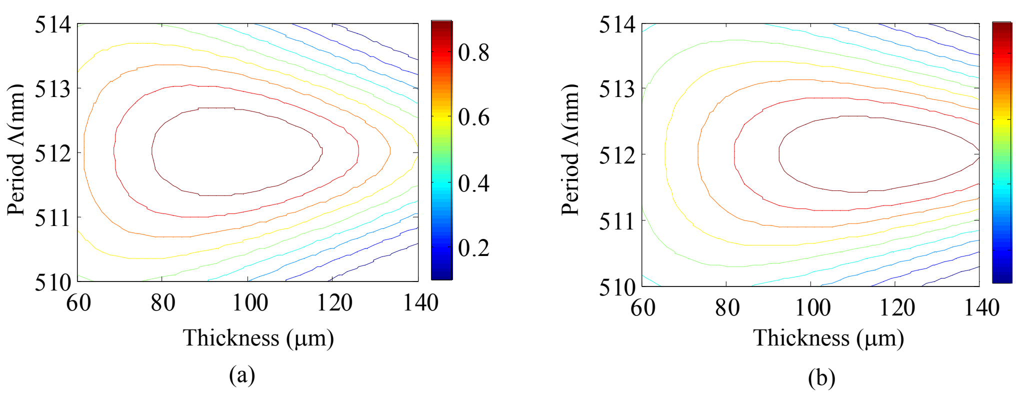


Fig.7 Diffraction efficiency depending on thickness *h* and period Λof grating for (a) TE- (b) TM-polarized

## 5. Multi-Points Side-Pumping

In this section, the multi-point side-pumping scheme is presented and the coupling and leaking efficiencies of pump powers are discussed when the high-power diode-bars multi-point side-pump DCF. The configuration of the multi-point side-pumping scheme is illustrated in Fig. 8. All the gratings have the same parameters as aforementioned.

As showed in Fig. 8, the diffracted pump lights 1$^{st}$ of the grating 1 is totally internal reflected at the interface of inner-outer cladding and incidents on the neighboring grating 2 at or near the angle of 82°. It may be diffracted again by the gratings 2. According to the coupled wave theory, the grating 2 should be regarded as a reflection grating due to the obliquity factor $c_S < 0$ when the 2nd diffraction occurs. Because the angle of incidence of the beam 1st is strongly violate the Bragg condition of the grating 2, the power of the diffracted beam 2nd_R is very weak while the power of the transmitting beam 2nd_T is just about the same of that of the beam 1st. The beam 2nd_T undergoes total internal reflection again at the interface of inner-outer cladding and continues to propagate in the DCF. Thus, the grating 2 can be regarded as a transparent zone for the diffracted lights 1st of the grating 1. The loss of the pump powers can be neglected even though the power of 2nd_R is totally leaked when DCF is multi-point side-pumped.

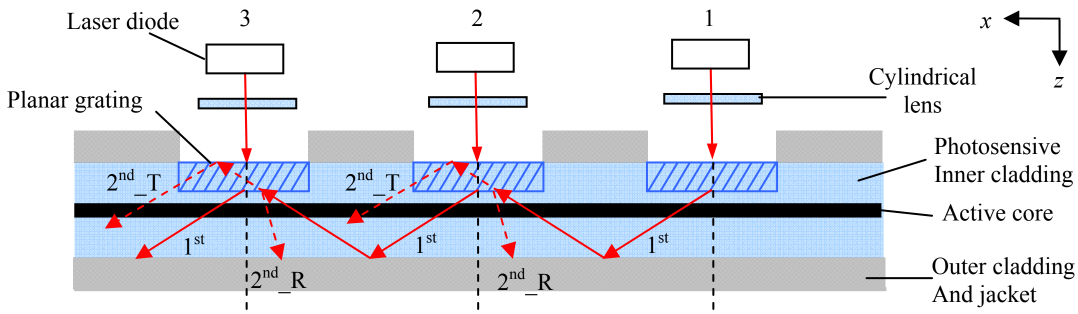


Fig.8 The multi-point side-pumping scheme through planar gratings

## 6. Conclusion

We presented an efficient and potential robust side-coupling scheme in this paper. The advantages of the scheme include: (1) no potential risk of damaging the DCF; (2) no optical adhesive; (3) high temperature sustainability; (4) simple, stable and integrated. And it is easy to scale the output power of the fiber lasers and amplifiers to very high powers by multi-point side-pumping. The simulation results show that with the proposed coupling structure it is possible to achieve over 98% coupling efficiencies for TE-, TM- and un-polarized incident pump lights simultaneously. Even when the pump wavelength ranges from 974.5 to 978.5*nm* and the incident angle ranges from $-0.8°$ to $0.8°$, the average diffraction efficiencies can still achieve 76.8% regardless of TE or TM polarization. A disadvantage of this side-pumping scheme is that the angular selectivity of the designed planar grating is a little narrow compared to the divergence angle of laser diode. It can be improved by changing the parameters of the planar grating, such as the thickness and the modulated amplitude of the refractive index of the inner cladding.

## Acknowledgment

This work was supported by the National Natural Science Foundation of China (No. 60678018) and the National Science Foundation for Post-doctoral Scientists of China (No. 20070420220 ).

## REFERENCES


[1]. Pan Ou, Ping Yan, Mali Gong, Wenlou Wei. Multi-coupler side-pumped Yb-doped double-clad fiber laser. Chinese Optics Letter, 2(5), 285~287 (2004).

[2]. Peterka P., Kasik I., Matejea V., *et al*. Novel coupling element for end-pumping double-clad fibers. in Proceedings of ECOC, Vol.3, 127~128 (2005).

[3]. Goldberg L., Cole B., Snitzer E.. V-groove side-pumped 1.5μm fibre amplifier. Electronics Letters, 33(25), 2127~2129 (1997).

[4]. Koplow J. P., Moore S. W., Kliner D. A. V.. A new method for side pumping of double-clad fiber source. IEEE Journal of Quantum Electronics, 39(4), 529~540 (2003).

[5]. Moore S. W., Koplow J. P., Hansen A., *et. al*. Embedded-mirror side pumping of double-clad fiber lasers and amplifiers. In proceeding of OSA/CLEO/QELS, (2008).

[6]. Hakimi F., Hakimi H.. A new side coupling method for double-clad fiber amplifier. In proceedings of CLEO, 116 (2001).

[7]. Lassila E., Hernberg R.. Axially symmetric fiber side pumping. Optics Express, 14(19), 8638~8643 (2006)
[8]. Kaneda Y., Mendes S. B., Jiang S.. Total internal reflection (VIR) coupler and method for side-coupling pump light into a fiber. United States Patent, US 6529318 B1 (2003).
[9]. Yan P., Gong M. L., Li C. *et al*.. Distributed pumping multifiber series fiber laser. Opt. Exp., 13(7), 2699～2706 (2005).
[10]. Herda R., Liem A., Schnabel B., *et. al*. Efficient side-pumping of fiber lasers using binary gold diffraction gratings. Electronics Letters, 39 (3), 276~277 (2003).
[11]. Zhang Fan, Wang Chuncan, Geng Rui, *et. al.*. Novel grating couplers for diode-bars multi-point side-pumping double-clad fiber. Optics Communications, 279, 346~355 (2007).
[12]. Zhang Fan, Wang Chuncan, Ning Tigang, *et. al*. Asymmetric dual-side-grating coupler for high power side-pumping. Optics Communications, 281, 2883~2892 (2008).
[13]. Yonghang Shen, Jinglei He, Tong Sun, *et. al*. High-temperature sustainability of strong fiber Bragg gratings written into Sb–Ge-codoped photosensitive fiber: decay mechanisms involved during annealing. Optics Letters, 29(6), 554~556 (2004).
[14]. Weizhong Zhao, Yonghang Shen, Tong Sun, et. al. FBGs in Bi-Ge co-doped photosensitive fibre for high temperature measurement up to 1000ºC. In proceedings of OSA/OFS, 2006
[15]. L. Dong, W. H. Loh, J. E. Caplen, et. al. Efficient single-frequency fiber lasers with novel photosensitive Er/Yb optical fibers. Optics Letters, 1997, 22(10): 694~696
[16]. K. Oh, J.M. Kim, H.S. Sco, et. al. Suppression of cladding mode coupling in Bragg grating using Ge2O-B2O3 codoped photosensitive cladding optical fibre. Electronics Letters, 1999, 35(5): 423~424
[17]. N. G. R. Broderick, D. J. Richardson, D. Taverner, et. al. High-power chirped-pulse all-fiber amplification system based on large-mode-area fiber gratings. Optics Letters, 1999, 24(8): 566~568
[18]. H. Kogenik. Coupled wave theory for thick hologram gratings. Bell Sys. Tech. J., 1969, 48(9): 2909~2946.